Int J Adv Manuf Technol (2016) 86:3113–3121
DOI 10.1007/s00170-016-8378-x

ORIGINAL ARTICLE

Kinematic analysis and experimental investigation on vibratory finishing

Y. B. Tian[1] · Z. W. Zhong[2] · S. J. Tan[2]

Received: 1 May 2015 / Accepted: 13 January 2016 / Published online: 10 February 2016

Abstract Vibratory finishing has been widely used for surface polishing, burnishing, edge finishing, texturing, and cleaning with a wide variety of different media. Medium properties and their motions dominate material removal efficiency and surface treatment quality in the vibratory finishing process. In this study, medium kinematic model and movement simulation of vibratory finishing were developed. Medium motion simulation was verified through a digit video recorded by a high-speed camera. It was found that medium kinematic path line is a circular-feeding helical motion, which is determined by the angular velocity ratio between the rolling and feeding, the rotation direction, and vibratory finishing machine configuration. Material removal intensity model was further established based on the kinematic model in order to better understand the vibratory finishing process. The optimal fixing location and orientation of workpiece were obtained through the analysis of the kinematic model. Finishing experiments were further carried out for the Ti6Al4V test pieces which were fixed onto the wall of a vibratory bowl. The surface roughness, Ra values (with initial surface roughness of 1.50 μm), approached to 0.13 μm after processing time of 2.5 h and 0.10 μm after processing time of 6.0 h. Surface quality of finished test pieces has been significantly improved as compared with the existing method (i.e., loosed workpiece in the vibratory bowl), whereby the surface roughness, Ra values (with initial surface roughness of 1.50 μm), tapered off (saturated) to about 0.52 μm with the increase of processing time.

Keywords Vibratory finishing · Kinematic motion · Material removal rate · Modeling · Media

✉ Y. B. Tian
ybtian@SIMTech.a-star.edu.sg; tyb79@sina.com

[1] Singapore Institute of Manufacturing Technology, 71 Nanyang Drive, Singapore 638075, Singapore

[2] School of Mechanical and Aerospace Engineering, Nanyang Technological University, 50 Nanyang Avenue, Singapore 639798, Singapore

1 Introduction

Vibratory finishing is a versatile surface treatment process that has been used for surface polishing, burnishing, edge finishing, texturing, strengthening, and cleaning/descaling during the past 50–60 years [1–3]. It is categorized into one of mass finishing processes, which is intent to modify surface properties of a part without affecting geometrical accuracy and bulk material properties. Hence, vibratory finishing is a typical near-net-shape surface modification and enhancement process. A vibratory finishing system usually consists of a spring-mounted open chamber/bowl containing granular media. A vibratory motion generator is attached to the chamber/bowl. The motion generator normally consists of one or two rotating shafts with eccentric weights [3–5]. A schematic diagram of typical vibratory finishing bowl system is shown in Fig. 1. Key vibratory finishing process variables include the frequency and amplitude of vibration; the amount and type of lubricant (also called "compounds" in mass finishing); and the size, shape, and properties of the media. The vibration amplitude and frequency of the finisher are controlled by adjusting the eccentric weight/configuration and the speed of the drive motor, respectively [1–3]. This makes the media become fluidized and generates complex flow fields within the chamber/bowl. The parts to be finished are entrained by the flowing media and experience a slower relative velocity. The media interact with the part surface through a combination of normal

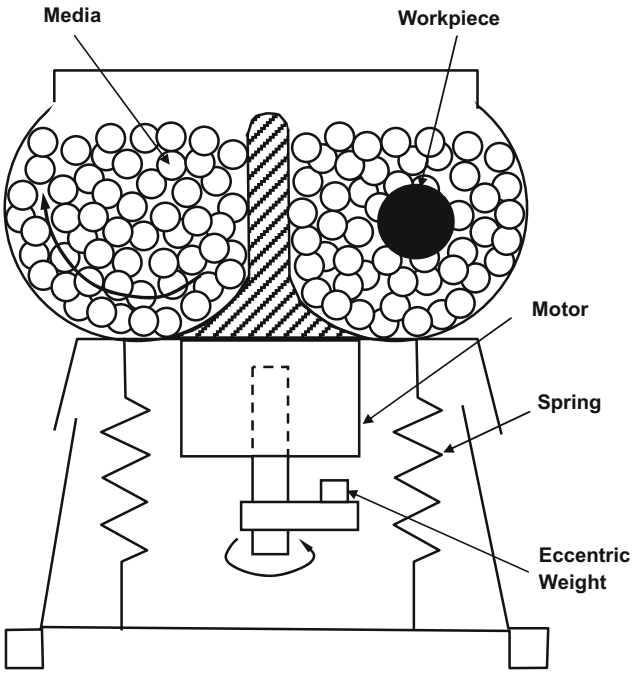

Fig. 1 Schematic diagram of typical vibratory finishing machine [4, 5]

impacts and tangential sliding. The process has been applied to metal, ceramic, and plastic parts, employing a wide variety of medium shapes and materials. The finishing media are currently used dry media or wet media with water-based lubricant [1, 3, 6, 7]. Typical media used in the vibratory finishing are shown in Fig. 2. Depending on the variation of the key process parameters, the vibratory finishing is capable of generating a wide range of contact conditions encompassing different degrees of rubbing, plowing, cutting, and three-body wearing behaviors [8].

While an extensive body of industrial experience and empirical information has been accumulated about its use during the past 50–60 years, fundamental knowledge of vibratory finishing with respect to medium motion, material removal, and surface modification has not been rigorously developed and finishing processes are largely developed through trial and error on the shop floor [1–8]. Relatively less scientific research has been reported with respect to vibratory finishing, and a few mathematical or process models exist [3]. Sofronas and Taraman [9] examined various finishing conditions to establish an empirical model of the vibratory finishing process as applied to the removal of surface material at edges. Hashimoto [10] carried out a series of experiments to determine the optimum finishing time for parts with different initial surface roughness. Mathematical modeling was developed to predict surface roughness and stock removal. The validity of the modeling was discussed with experimental results, and an algorithm to design an optimum process of vibratory finishing was proposed. Domblesky and Cariapa et al. [11] conducted an experimental investigation into the vibratory bowl finishing process using material removal rate and surface roughness as the dependent variables. It was found that bowl performance could best be described in terms of acceleration and depended primarily on the feed weights used, while bowl loading had a relatively minor effect. Furthermore, small changes in bowl loading resulting from normal medium wear could be neglected. Results showed that material removal rates were constant over time for aluminum, brass, and steel and were sensitive to hardness and bowl acceleration. Surface roughness saturated after a fixed period and was primarily a function of material composition. Surface roughness did not appear to be sensitive to bowl acceleration. Domblesky and Evans et al. [4] further develop a model to describe mass removal rate in vibratory finishing as a function of bowl acceleration, workpiece mass, velocity, and specific energy. The model indicates that the material removal rate remains constant over time (8 h) and is governed by bowl acceleration, workpiece mass, material properties, and workpiece velocity. Results from controlled experimental testing using an instrumented vibratory bowl indicate that their model provides a reasonable representation of the governing process variables. Uhlmann and Dethlefs [12] proposed a new approach, i.e., geometric modeling of vibratory finishing process to predict surface roughness variation after a given process time. In contrast to other simulation approaches concentrating on mass or diameter loss of the workpiece, this approach is based on geometric changes of the roughness profile during the transient period of vibratory finishing. The model can be used to estimate processing time needed to achieve a desired surface roughness of a workpiece. The model is based on the hypothesis that, during transient period, material removal rate is proportional to the improvement in surface roughness. Similarly, empirical modeling and finite element modeling and simulation were also adopted in other mass finishing process such as centrifugal disk finishing [13]. Matsunaga [13] presented a theoretical model and related experimental investigation on centrifugal disk finishing. A calculation for the centrifugal force in the barrel was described. The limitation of the ratio between the rotation speed of the tub and the turret and the value of finishing efficiency were determined by both the theoretical calculation and the experimental results. This study explained why the finishing efficiency of the centrifugal disk finishing was far higher than that of the ordinary rotary barrel finishing. In order to describe kinematic movement and flow of medium particles in a centrifugal disk, Cariapa and Park et al. [14] developed a finite element method (FEM) model of the flow pattern of media moving in the centrifugal disk system when the moving medium was assumed as a fluid. Via experimentally determined properties of a pseudo-fluid (i.e., mass density and absolute viscosity), fluid dynamic theories were employed to predict the velocity profiles in the system using commercially available software, FLUENT. The computer-generated path lines of flowing particles were obtained through the FEM simulation. The planar velocity of the

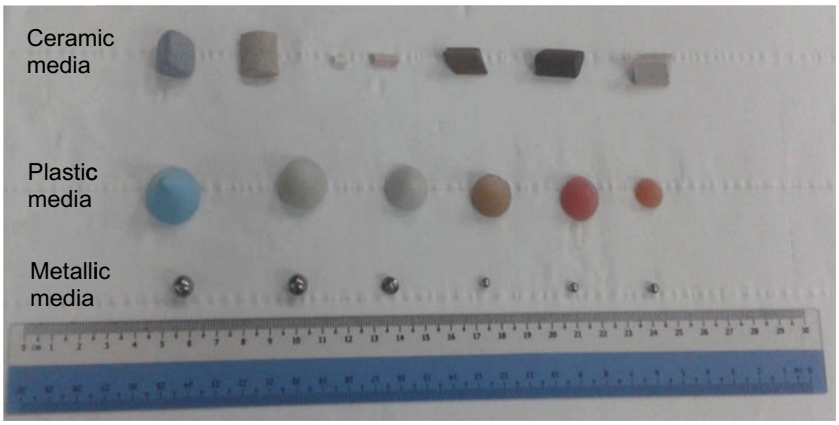

Fig. 2 Typical media with different materials, shapes, and sizes used in vibratory finishing

moving media obtained by experimental measurement and numerical model was compared in order to corroborate the validity of theoretical model.

More recently, great efforts have been made to explore vibratory finishing mechanism and optimize process conditions through process monitoring and experimental investigation. Wang and Timsit et al. [15] measured the distribution of normal contact force over processing time per unit surface area of a force sensor placed in a bowl-type vibratory finisher. The resulting changes were compared in terms of surface roughness and hardness of two aluminum alloys, namely, AA1100-O and AA6061-T6. It was observed that the principal variables were the medium size, degree of lubrication, and duration of the vibratory finishing. The changes in hardness and roughness of the finished test coupons were found to depend mostly on the lubrication condition and the size of the media, which influenced the interaction between the media and the workpiece, and hence the extent of plastic surface deformation per impact. However, impact force did not appear to vary significantly with medium size or lubrication conditions. Thus, the differences observed in hardness and roughness were apparently due to smaller-scale differences in the impact contact conditions [15]. Video camera observations showed that the media were loosely packed as they flowed past the workpiece, with relatively large gaps in the packing near the workpiece surface. Furthermore, impact craters reflected the dominance of normal impact in dry conditions and sliding in wet conditions. Yabuki and Baghbanan et al. [16–18] measured both the normal and tangential contact forces in the same bowl-type vibratory finishing machine. Together with a video system, it was established that collisions between the finishing media and the test coupon surface occurred in three different modes. The ratio of the normal and tangential forces was compared with the measured friction coefficient under dry and water-wet conditions, confirming that medium sliding occurred under

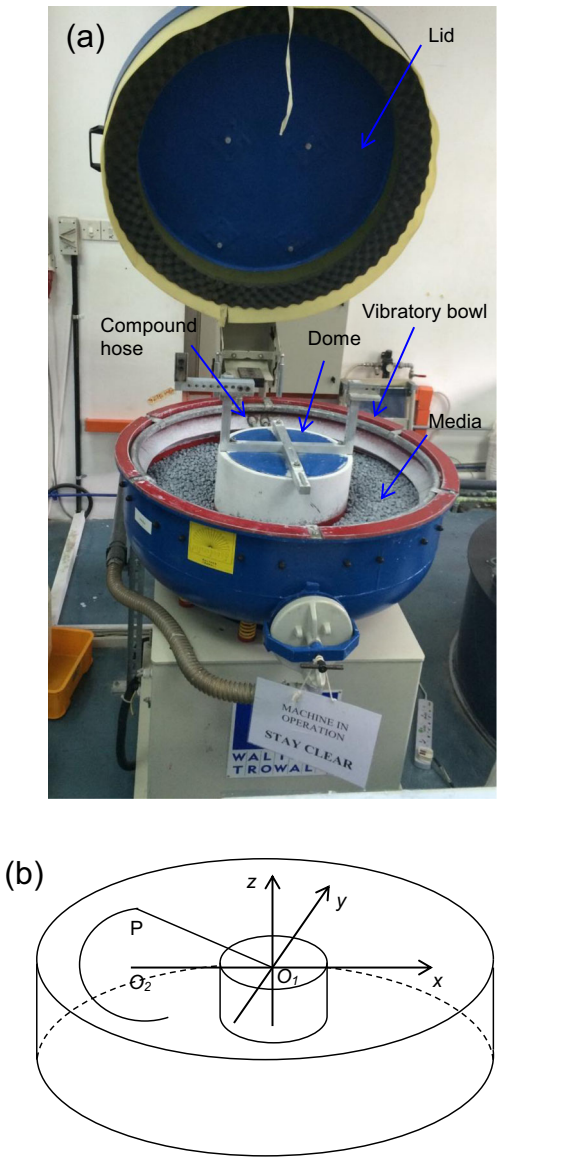

Fig. 3 **a** Vibratory bowl-type finishing system filled with ceramic media. **b** Schematic diagram of established *x*-*y*-*z* coordinate system on bowl-type finishing system

water-wet conditions. Ciampin and Papini [19] measured surface normal impact velocity distributions, impact frequencies, and impact power per unit area using a force sensor in a vibratory finisher for two types of spherical media. These parameters control the degree, rate and character of plastic deformation, and erosion of a workpiece surface in vibratory finishing. The force sensor was also used to quantify the effect of medium type, finisher amplitude, and location within the finisher on the probability distribution of the particle impact velocity normal to the workpiece. Most aggressive finishing conditions were determined through the process monitoring. The Almen system was further adapted to a vibratory finishing process to characterize the effect of varying process parameters for the purposes of process development and control [20]. Saturation curves for two types of aluminum Almen strips were obtained by finishing at two distinct conditions using a trough-type vibratory finisher and steel spherical media. Comparison with the normal contact forces and effective impact velocities measured for both these conditions provided deep insight into the mechanics of the vibratory finishing process [20]. Kumar and Sathyan [21] measured the contact forces in one-dimensional vibratory finishing machine using multi-body dynamic software. A vibratory simulator was modeled via SolidWorks, and the model was imported into commercial multi-body dynamic software, RecurDyn, to obtain the contact force of the media and the workpiece. A series of experiments were performed in a one-dimensional vibration shaker. The peak force signal with respect to time was recorded and compared with simulation results. Wan and Sato et al. [22] monitored impact forces in a bowl-type vibratory finishing machine with a force sensor and conducted vibratory finishing investigation on immobilized cylinders with a cantilever fixture. It was mentioned that the vibration of fixture would accelerate the interaction of media and workpiece. From currently existing knowledge of vibratory finishing, the material removal mechanism, medium motion, and high efficiency finishing strategy remain unclear. In order to reduce trial and error on the shop floor, it is essential to further understand the vibratory finishing process and develop the theoretical model of material removal. In this work, we started from the development of medium kinematic model and simulation of vibratory finishing. Material removal intensity model was then established through the kinematic model for the vibratory finishing. Based on the findings from the theoretical model, high-efficiency finishing with good quality was eventually attained.

2 Kinematic model and simulation

2.1 Theoretical model for medium motion

In vibro bowl finishing system, media flow inside a circle bowl. A typical vibratory bowl-type finishing system structure filled with ceramic media (Walter Trowal CM-205) is shown in Fig. 3a. It should be noted that motor, eccentric weight, and spring are covered below the medium bowl. The movement of a medium (or loose workpiece) of the vibratory bowl

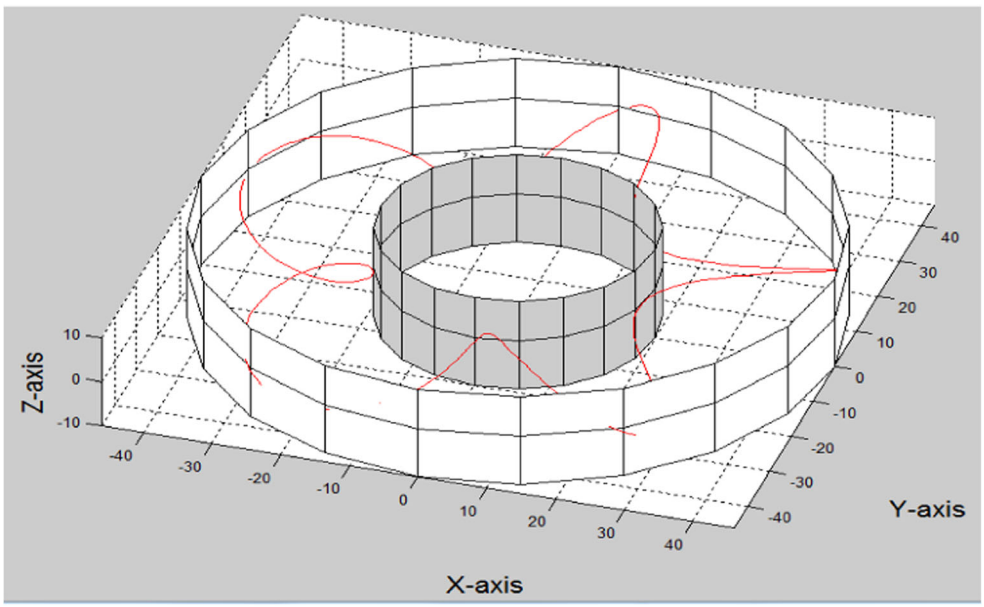

Fig. 4 Helical motion of a medium during vibratory finishing ($\omega_x = 5$, $\omega_1 = \frac{\pi}{3}$, $\omega_2 = \frac{\pi}{15}$, $e = 330$ mm, and $r_1 = 130$ mm; $r_2 = 75$ mm)

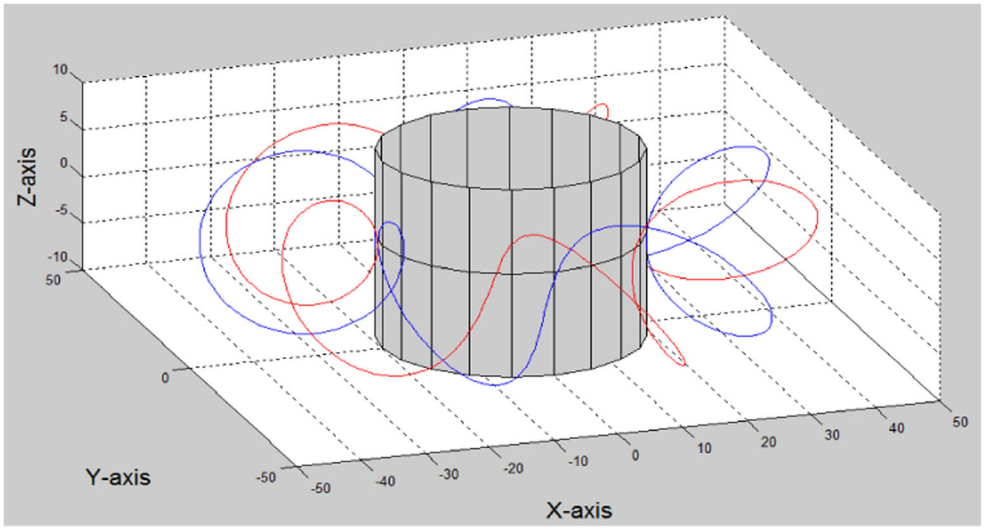

Fig. 5 Helical motion of two media in vibratory bowl ($\omega_x = 5$, $\omega_1 = \frac{\pi}{3}$, $\omega_2 = \frac{\pi}{15}$, $e = 330$ mm, and $r_1 = 130$ mm; $r_2 = 75$ mm)

system is generated as the combination of rolling and feeding around the bowl dome center. An *x*-*y*-*z* coordinate system is set in which *x* axis is defined as O_1O_2 (bowl center (O_1) and rolling center (O_2)), and its origin O_1 was fixed at the axis of dome center, as illustrated in Fig. 3b. A parametric equation of the kinematic trajectory of a point (*P*) on a medium relative to the stationary bowl can be described as

$$\begin{cases} x = [e + r_1 \sin(\omega_1 \cdot t)] \cdot \cos(\omega_2 \cdot t) \\ y = [e + r_1 \sin(\omega_1 \cdot t)] \cdot \sin(\omega_2 \cdot t) \\ z = r_2 \cos(\omega_1 \cdot t) \end{cases} \quad (1)$$

where *x*, *y*, and *z* are the coordinates of the medium point on the trajectory; ω_1 is the angular velocity of the medium rolling; ω_2 is the angular velocity of the medium feeding around the bowl center; *e* is the center distance between the bowl center (O_1) and the rolling center (O_2); r_1 is the long elliptical axis and r_2 is the short elliptical axis; and *t* is the finishing time.

The kinematic curve of the medium is a circular-feeding helical motion. If ω_x is defined as the angular velocity ratio between the rolling and feeding, i.e., $\omega_x = {}^{\omega_1}/_{\omega_2}$. If substituting $\omega_x = {}^{\omega_1}/_{\omega_2}$ and $t = \theta/\omega_1$ (θ is the rolling angle) into Eq. (1), the expression of the medium trajectory equation can be rewritten as

$$\begin{cases} x = [e + r_1 \sin\theta] \cdot \cos\left({}^{\theta}/_{\omega_x}\right) \\ y = [e + r_1 \sin\theta] \cdot \sin\left({}^{\theta}/_{\omega_x}\right) \\ z = r_2 \cos\theta \end{cases} \quad (2)$$

Therefore, when vibratory finishing machine configuration is fixed, the kinematic trajectory is only determined by the angular velocity ratio and the rotation direction, regardless of the individual value of the angular velocity.

According to the configuration of the current set of the Walter Trowal CM-205 vibratory bowl, as shown in Fig. 3a, $\omega_x = 5$ ($\omega_1 = \frac{\pi}{3}$; $\omega_2 = \frac{\pi}{15}$ from experiment measurement when vibration amplitude is 4 mm, vibratory lead angle is 80°, and vibration frequency is 40 Hz), the center distance between the bowl center (O_1) and the rolling center (O_2), *e* is 330 mm. The long elliptical axis r_1 and the short elliptical axis r_2 are 130 and 75 mm, respectively. The parametric equation of the kinematic trajectory can be expressed as

$$\begin{cases} x = [330 + 130\sin\theta] \cdot \cos\left({}^{\theta}/_{5}\right) \\ y = [330 + 130\sin\theta] \cdot \sin\left({}^{\theta}/_{5}\right) \\ z = 75 \cos\theta \end{cases} \quad (3)$$

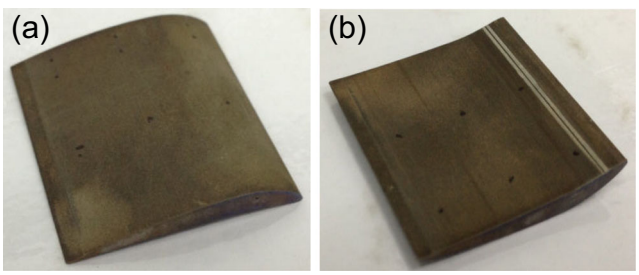

Fig. 6 Fabricated Ti64 test pieces with designed geometry, **a** convex side and **b** concave side

Fig. 7 Straight-cut triangular (*F*-triangle) ceramic media used

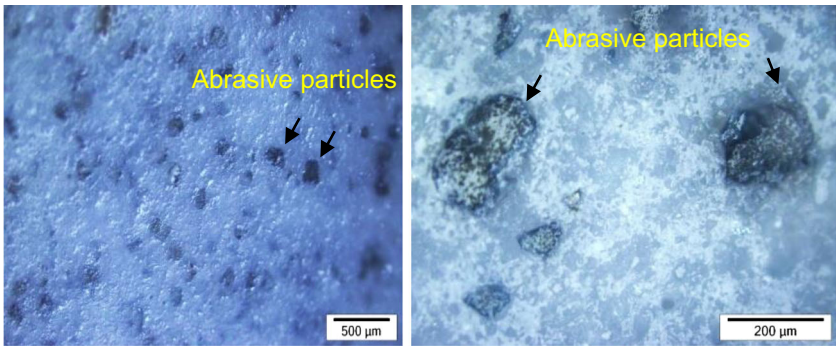

Fig. 8 Surface topography of straight-cut triangle (*F*-triangle) ceramic media

Based on Eq. (3), the loci of a medium and two media during vibratory finishing are plotted in Figs. 4 and 5, respectively.

2.2 Theoretical model for material removal intensity

Using Eq. (1), the parametric equation of the relative velocity of a point (*P*) on a medium (or loose test piece) can be found as follows:

$$\begin{cases} v_x = \dfrac{\delta_x}{\delta_t} = r_1\omega_1\sin(\omega_1 \cdot t)\cdot\cos(\omega_2 \cdot t) - [e\omega_2 + r_1\omega_2\sin(\omega_1 \cdot t)]\cdot\sin(\omega_2 \cdot t) \\ v_y = \dfrac{\delta_y}{\delta_t} = r_1\omega_1\sin(\omega_1 \cdot t)\cdot\sin(\omega_2 \cdot t) + [e\omega_2 + r_1\omega_2\sin(\omega_1 \cdot t)]\cdot\cos(\omega_2 \cdot t) \\ v_z = \dfrac{\delta_z}{\delta_t} = - r_2\omega_1 \cdot \sin(\omega_1 \cdot t) \end{cases} \quad (4)$$

As the relative velocity of the point (*P*) on the medium is $v = \sqrt{v_x^2 + v_y^2 + v_z^2}$, its value can be re-described using Eq. (4).

$$v = \sqrt{\left(r_1^2 + r_2^2\right)\cdot\omega_1^2\cdot\sin^2(\omega_1 \cdot t) + [e\cdot\omega_2 + r_1\cdot\omega_2\sin(\omega_1 \cdot t)]^2} \quad (5)$$

Next, by rewriting the well-known law for two- and three-body wear $v_s = (k_s \cdot W \cdot L)/H$ as the wear depth (i.e., material removal intensity) h_s,

$$h_s = (k_s \cdot P_a \cdot v) \Big/ H \quad (6)$$

where k_s is the wear coefficient, W is the normal load, H is the hardness of test piece, v is the sliding velocity, P_a is the apparent pressure, and $L = v \cdot t$.

For a vibratory bowl-type finishing machine, the center distance between the bowl center and the rolling center is usually fixed. Meanwhile, the amplitude and frequency of the vibratory finisher will be set, when the eccentric weight or the speed of the drive system is adjusted. According to Eqs. (5) and (6), the long elliptical axis r_1 and the short elliptical axis r_2 values are determined by media (or workpiece) positions. If the workpiece is far from the rolling center, the relative velocity will achieve maximum value and material removal intensity. Hence, fixing of workpiece onto the wall of vibratory bowl was further recommended and tested in order to attain high-efficiency vibratory finishing.

3 Experimental details

3.1 Material and workpiece

Titanium alloys have received considerable interest recently due to their wide range of applications in the aerospace, automotive, chemical, and medical industries [3, 22–25]. They exhibit good compromise between density and yield strength and also have good creep and fatigue resistance at midtemperatures [25, 26]. However, titanium alloys are considered to be difficult to machine due to high chemical reactivity, relatively low thermal conductivity, and low modulus of elasticity [22–26]. Vibratory finishing or other surface finishing processes are usually required to deburr and improve surface integrity after mechanical cutting [26].

In this investigation, the material of workpiece is selected as Ti6Al4V (Ti64). This material is the most common titanium alloy, belongs to α + β alloy group, and accounts for more

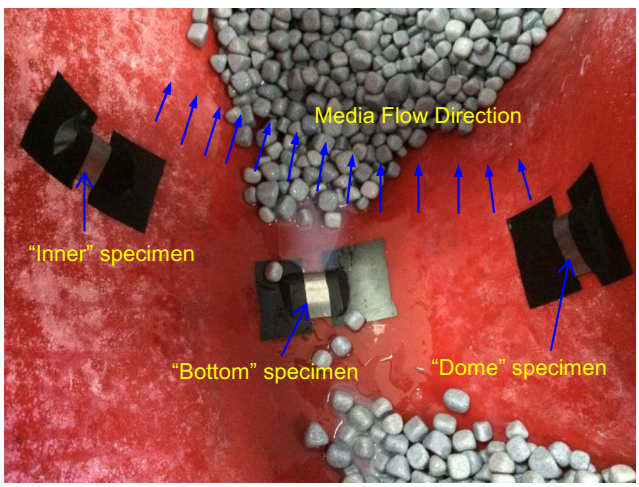

Fig. 9 Specimen locations inside vibratory finishing bowl

Table 1 Vibratory finishing condition

Media	Compound	Motor rotation RPM	Flywheel setting	Vibration amplitude	Vibration lead angle
F-triangle	5 % ARF fluid	1500	20 mm	4 mm	80°

than 50 % of the titanium alloy production [26]. The material modulus is 110 GPa, and tensile strength is 860–965 MPa [26]. Workpieces were fabricated with specially designed freeform surface with concave and convex geometries, as shown in Fig. 6.

3.2 Finishing experiments and assessments

3.2.1 Medium flow motion verification

Walter Trowal CM-205 vibratory finisher with 1100-mm polyethylene bowl in diameter was used to carry out experiments, in order to verify the medium flow motion simulation results presented in Figs. 4 and 5. The usable bowl capacity was 110 L. A vibratory motion generator is attached to the vibratory bowl. The motion generator consists of one rotating shaft with eccentric weights. The vibration amplitude of 4.0 mm, vibratory lead angle of 80° (clockwise flow direction), and vibratory frequency of 45 Hz were adjusted in this work. Straight-cut triangular (*F*-triangle) ceramic media with dimension of 13 × 13 mm were employed. The photograph of the typical media used was shown in Fig. 7. The ceramic media comprise of abrasive particles and bonding materials. The typical medium surface topography observed with optical microscope was shown in Fig. 8. The media were filled with the bowl during the experiments. Compound of 5 % Trowal™ ARF fluid diluted with 95 % DI water was used as lubrication. The fluid flow rate was selected as ~200 ml/min. One medium was purposely dyed with dark color. A video of the medium flow pathway was recorded with a high-speed digital camera. The results were compared with medium motion simulated.

3.2.2 Fixed workpiece experiments

From the material removal model in this study, the maximum relative velocity and higher pressure were generated when workpiece was close to the wall of the vibratory bowl. Hence, the designed Ti6Al4V (Ti64) workpieces were fixed onto the wall of the Walter Trowal CM-205 vibratory bowl, three locations, namely, bottom bowel, inner dome, and outer bowel, which were further tested with same initial surface roughness of 1.5 μm, as illustrated in Fig. 9. The finishing results were compared with conventional finishing method, i.e., test piece without any immobilization (loosed test piece inside the vibratory bowl), under the same finishing conditions. The vibratory finishing conditions were shown in

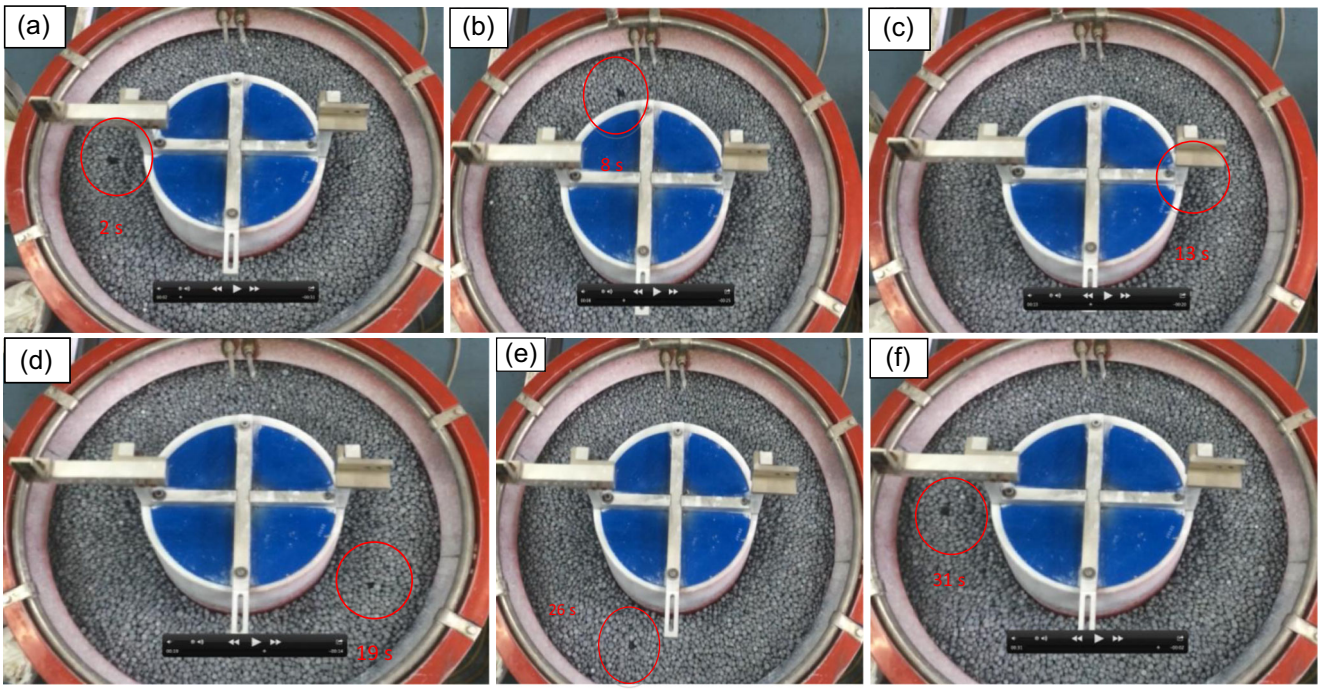

Fig. 10 Recorded motion of the dark media dyed at different times, **a** 2 s, **b** 8 s, **c** 13 s, **d** 19 s, **e** 26 s, and **f** 31 s

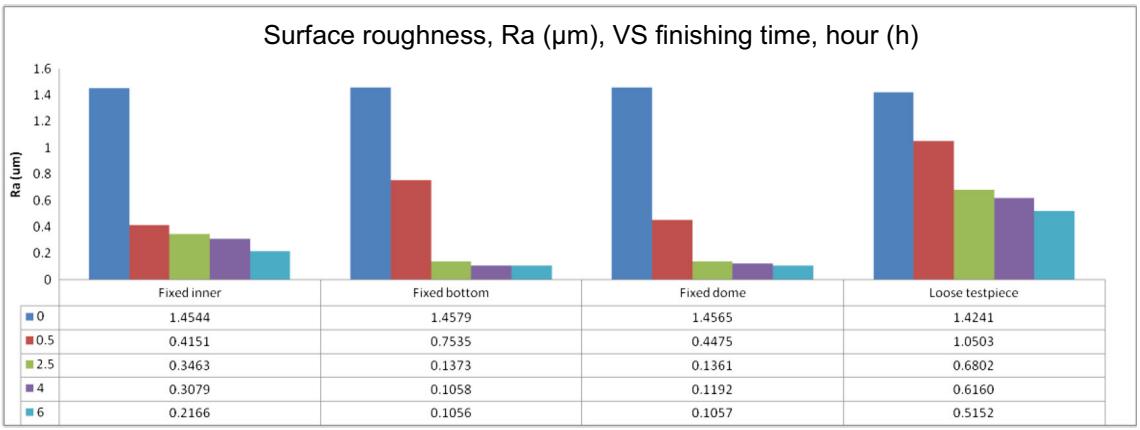

	Fixed inner	Fixed bottom	Fixed dome	Loose testpiece
0	1.4544	1.4579	1.4565	1.4241
0.5	0.4151	0.7535	0.4475	1.0503
2.5	0.3463	0.1373	0.1361	0.6802
4	0.3079	0.1058	0.1192	0.6160
6	0.2166	0.1056	0.1057	0.5152

Fig. 11 Comparison of surface roughness of specimens being finished with loose test piece and fixed test piece onto different locations

Table 1. Each test piece was finished for total of 180 min. The processing times were 30 min, 2.5, 4, and 6 h. After each finishing test, surface roughness, arithmetic mean roughness (Ra), was measured with Stylus profilometer to evaluate finishing performance.

4 Results and discussion

4.1 Verification for medium flow path

Figure 10 shows the video recorded position of the dyed media inside the Walter Trowal CM-205 vibratory bowl at different times of 2, 8, 13, 19, 26, and 31 s, respectively. When the same conditions and configurations were selected, i.e., the angular velocity ratio of 5 and the clockwise rotation direction, the center distance between the bowl center and the rolling center was 330 mm, and the long elliptical axis and the short elliptical axis were 130 and 75 mm, respectively, it was observed that the motion of the recorded medium matched well with the simulation.

4.2 Experimental results for fixed workpiece

Figure 11 shows the comparison of arithmetic mean roughness (Ra) of the finished specimens at different processing time under the conditions of loose test piece and fixed test piece onto "bottom bowl," "inner dome," and "outer bowl," respectively. The surface roughness decreased with the increase of the processing time for both loose test piece and novel fixed test piece. The roughness changing rate was gradually reduced as the roughness approached the roughness limitation (final roughness value). It can be seen that the Ra values of fixed test pieces are much less (better) than those of loosed test piece (i.e., existing vibratory finishing method) under the same finishing condition. The Ra value of the loosed test piece gradually saturated to 0.52 μm after accumulative vibratory finishing time of 6 h, while the Ra values of the fixed test pieces onto the bowl wall achieved less than 0.22 μm after the same processing time. Especially, the Ra values almost approached to 0.13 μm after processing time of 2.5 h and 0.10 μm after processing time of 6 h when the test pieces were fixed on bottom bowl and inner dome, respectively. As shown in Fig. 12, the unfinished test piece was quite rough, while test piece fixed on the inner dome became specular after being finished for 2.5 h. It was found that test piece fixed onto the bottom bowl of vibratory finisher attained the least (best) surface roughness.

In mass finishing process, materials are usually removed without affecting geometrical accuracy and bulk material properties, i.e., near-net-shape surface finishing. During transient period in vibratory finishing, material removal rate is proportional to the improvement in surface roughness [1, 2, 13]. In another word, the larger reduction in surface roughness

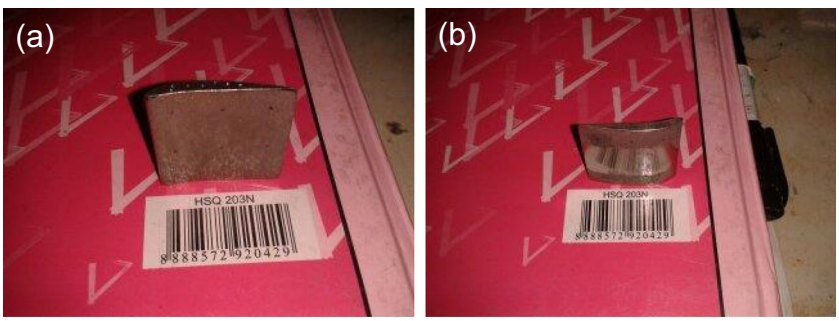

Fig. 12 **a** Unfinish test piece and **b** after finishing for 2.5 h

indicated more aggressive material removal. When test piece was fixed onto the bottom bowel of vibratory finisher, maximum relative velocity and higher pressure were generated as explained in material removal intensity (Eqs. (4))–(6)). In addition, the direct attachment of the workpieces to the bowl wall would also avoid the energy loss transmitted from the motor. The interaction between media and media would lose energy and mitigate the effective impact velocity, although medium contacts occur periodically within time periods that correspond to the finisher's driving frequency [19]. Hence, direct attachment of the workpiece to the wall of the vibratory bowl, such as bottom bowl and inner dome, could realize high efficiency while maintaining good surface quality.

5 Concluding remarks

In this work, material removal mechanism of vibratory finishing was revealed through kinematic model and simulation. The kinematic curve of media in vibratory finisher is a circular-feeding helical path which is determined by the angular velocity ratio between the rolling and the feeding, the rotation direction, and vibratory finishing machine configuration. Material removal intensity was developed based on the kinematic model. It was concluded that the relative velocity and material removal intensity would achieve the maximum value when test piece is fixed far from the rolling center, such as bottom bowl and inner dome. The medium motion model was verified through a digit video recorded by a high-speed camera. Finishing experiments were further carried out for test pieces fixed onto the wall of vibratory bowl. Surface roughness, Ra values with initial surface roughness of 1.5 μm, approached to 0.13 μm after processing time of 2.5 h and 0.10 μm after processing time of 6 h. Surface quality of finished components has been significantly improved as compared with the existing method (i.e., loose workpiece), whereby the surface roughness, Ra values (with initial surface roughness of 1.5 μm), saturated to about 0.52 μm with the increase of processing time.

Acknowledgments This research was financially sponsored by the Agency for Science, Technology and Research of Singapore via Singapore Institute of Manufacturing Technology (SIMTech) Project Grant C12-M-047.

References

1. Gillespie LRK (2006) Mass finishing handbook. Industrial Press Inc, New York
2. Gillespie LRK (1999) Deburring and edge finishing handbook. ASME, New York
3. Mediratta R, Ahluwalia K, Yeo SH (2015) State-of-the-art on vibratory finishing in the aviation industry: an industrial and academic perspective. Int J Adv Manuf Technol. doi:10.1007/s00170-015-7942-0
4. Domblesky J, Evans R, Cariapa V (2004) Material removal model for vibratory finishing. Int J Prod Res 42:1029–1041
5. Ciampinia D, Papinib M, Spelta JK (2009) Modeling the development of Almen strip curvature in vibratory finishing. J Mater Process Technol 209:2923–2939
6. Kenton T (2009) The future of mechanical surface finishing. Met Finish 107:22–24
7. Davidson DA (2007) Green mass finishing with dry abrasive and polishing media. Met Finish 105:45–48
8. Marinescu ID, Rowe WB, Dimitrov B, Inasaki I (2004) Tribology of abrasive machining processes. William Andrew, Inc, New York
9. Sofronas A, Taraman S (1979) Model development and optimization of vibratory finishing process. Int J Prod Res 17:23–31
10. Hashimoto F (1996) Modeling and optimization of vibratory finishing process. CIRP Ann- Manuf Technol 45:303–306
11. Domblesky J, Cariapa V, Evans R (2003) Investigation of vibratory bowl finishing. Int J Prod Res 41:3943–3953
12. Uhlmann E, Dethlefs A, Eulitz A (2014) Investigation into a geometry-based model for surface roughness prediction in vibratory finishing processes. Int J Adv Manuf Technol 75:815–823
13. Matsunaga M (1967) Theory and experiments on centrifugal barrel finishing. Int J Prod Res 5:275–287
14. Cariapa V, Park H, Kim J, Cheng C, Evaristo A (2008) Development of a metal removal model using spherical ceramic media in a centrifugal disk mass fishing machine. Int J Adv Manuf Technol 39:92–106
15. Wang S, Timsit RS, Spelt JK (2000) Experimental investigation of vibratory finishing of aluminum. Wear 243:147–156
16. Yabuki A, Baghbanan MR, Spelt JK (2002) Contact forces and mechanisms in a vibratory finisher. Wear 252:635–643
17. Baghbanan MR (2002) Contact forces and surface characterization of aluminum alloys in a vibratory surface finishing process, M. Sc. thesis, University of Toronto
18. Baghbanan MR, Yabuki A, Timsit RS, Spelt JK (2003) Tribological behaviour of aluminum alloys in a vibratory finishing process. Wear 255:1369–1379
19. Ciampini D, Papini M, Spelt JK (2007) Impact velocity measurement of media in a vibratory finisher. J Mater Process Technol 183: 347–357
20. Ciampini D, Papini M, Spelt JK (2008) Characterization of vibratory finishing using the Almen system. Wear 264:671–678
21. Kumar PP, Sathyan S (2012) Simulation of 1D abrasive vibratory finishing process. Adv Mater Res 565:290–295
22. Wan S, Sato T, Hartawan A (2012) Vibratory finishing of immobilized cylinders. Adv Mater Res 565:278–283
23. Boyer RR (1996) An overview on the use of titanium in the aerospace industry. Mater Sci Eng A 213:103–114
24. Pujana J, Rivero A, Celaya A, Lacalle LNL (2009) Analysis of ultrasonic-assisted drilling of Ti6Al4V. Int J Mach Tools Manuf 49:500–508
25. Ohkubo C, Hosoi T, Ford JP, Watanabe I (2006) Effect of surface reaction layer on grindability of cast titanium alloys. Dent Mater 22: 268–274
26. Axinte DA, Kwong J, Kong MC (2009) Workpiece surface integrity of Ti-6-4 heat-resistant alloy when employing different polishing methods. J Mater Process Technol 209:1843–1852